Cancer Cell
Article

Mosaic Amplification of Multiple Receptor Tyrosine Kinase Genes in Glioblastoma

Matija Snuderl,[1,6] Ladan Fazlollahi,[1,6] Long P. Le,[1] Mai Nitta,[1] Boryana H. Zhelyazkova,[1] Christian J. Davidson,[1] Sara Akhavanfard,[1] Daniel P. Cahill,[2,4] Kenneth D. Aldape,[3,4] Rebecca A. Betensky,[5] David N. Louis,[1] and A. John Iafrate[1,*]
[1]Department of Pathology, Massachusetts General Hospital and Harvard Medical School, Boston, MA 02114, USA
[2]Department of Neurosurgery
[3]Department of Pathology
[4]MD Anderson Cancer Center, Houston, TX 77030, USA
[5]Department of Biostatistics, Harvard School of Public Health, Boston, MA 02115, USA
[6]These authors contributed equally to this work
*Correspondence: aiafrate@partners.org
DOI 10.1016/j.ccr.2011.11.005

SUMMARY

Tumor heterogeneity has been implicated in tumor growth and progression as well as resistance to therapy. We present an example of genetic heterogeneity in human malignant brain tumors in which multiple closely related driver genes are amplified and activated simultaneously in adjacent intermingled cells. We have observed up to three different receptor tyrosine kinases (*EGFR*, *MET*, *PDGFRA*) amplified in single tumors in different cells in a mutually exclusive fashion. Each subpopulation was actively dividing, and the genetic changes resulted in protein production, and coexisting subpopulations shared common early genetic mutations indicating their derivation from a single precursor cell. The stable coexistence of different clones within the same tumor will have important clinical implications for tumor resistance to targeted therapies.

INTRODUCTION

Tumor heterogeneity is defined by the presence of cell subpopulations harboring distinct genetic or gene expression profiles with distinct biologic properties (Marusyk and Polyak, 2010) and plays a crucial role in tumor progression and resistance to therapy (Gerlinger and Swanton, 2010). Studies have shown that tumor heterogeneity affects most critical tumor properties such as metastatic potential (Yachida et al., 2010), acquired resistance to therapy (Yip et al., 2009), and angiogenic potential (Jain et al., 2007). Whereas regional genetic heterogeneity within single tumors is well-described and termed clonal evolution, it is generally assumed that pro-growth changes accumulate within a tumor cell and lead to evolution of the most viable clone.

Glioblastoma (GBM) is the most common malignant brain tumor of adults (Louis et al., 2007), with poor prognosis regardless of treatment (Nicholas, 2007). Amplification of receptor tyrosine kinase (RTK) genes plays a crucial role in tumorigenesis of GBM and is a major driver of tumor growth through activation of the mitogen-activated protein kinase pathway. Up to 50% of GBMs have amplification of an RTK, including *EGFR*, *KIT*, *VEGFR2*, *PDGFRA*, and *MET* (Joensuu et al., 2005; Puputti et al., 2006; Wullich et al., 1993). High-level amplification of RTK genes appears to be a relatively late event in the tumorigenesis of GBM (Attolini et al., 2010), and usually only one RTK shows high level amplification. We present here a study of malignant human brain tumors in which we examined the distribution of *EGFR*, *MET*, and *PDGFRA* amplification events in situ to assess the degree of tumor heterogeneity and to identify tumors with coamplification of multiple RTKs.

RESULTS

Simultaneous Amplification of Multiple RTKs in GBM

With the purpose of identifying RTKs as possible novel therapeutic targets in GBM, we analyzed the Cancer Genome Atlas project copy number data for amplifications of specific RTKs

Significance

Tumor heterogeneity plays a major role in tumor growth and progression and largely contributes to therapy resistance. We present a subset of malignant brain tumors with genetic heterogeneity in the form of intermingled populations of tumor cells containing amplification of different receptor tyrosine kinase genes. We show that each population is viable and participates in the growth of the tumor and that all clones share early genetic changes confirming an origin from a common precursor. Our study provides important insight into the complexity of tumor heterogeneity and has important implications for targeted therapy.

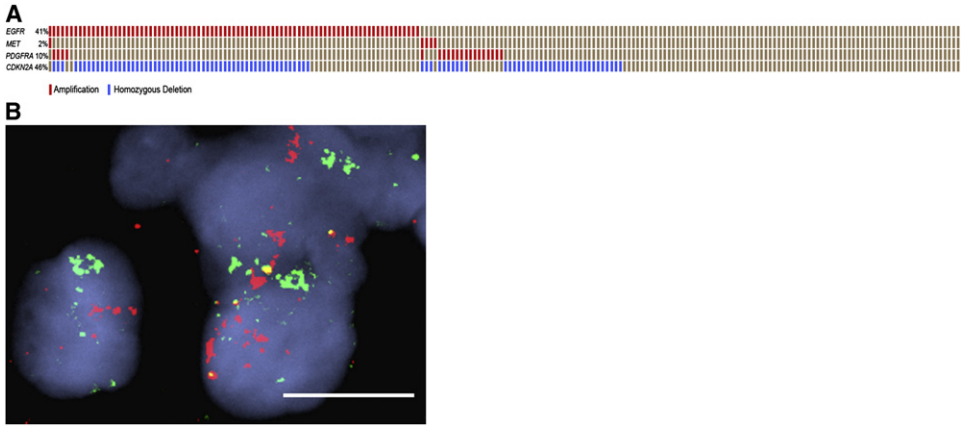

Figure 1. Data Obtained from Analyses of TCGA Copy Number in GBM

(A) Detailed view of *EGFR*, *MET*, and *PDGFRA* amplification and homozygous deletions of *CDKN2A*. Cases are arranged so that each column represents single cases (see Figure S1 for complete receptor tyrosine kinase data).

(B) FISH analysis of TCGA-02-0024 case shows amplification of *MET* (green) and *PDGFRA* (red) in the same tumor cells. Scale bar, 20 μm.

(Cancer Genome Atlas Research Network, 2008). Out of 206 cases, approximately 50% of GBMs showed amplification of at least one of the 51 RTKs investigated (Figure S1 available online). The most commonly amplified RTK gene was *EGFR* (41% of the cases) followed by *PDGFRA* (10%), which is commonly coamplified with *KIT* (7% of the cases) and *KDR* (4% of the cases) as a part of a single 4q12 amplicon (Joensuu et al., 2005; Puputti et al., 2006). *MET* was the third most commonly amplified RTK (2% of the cases). Seven other RTKs showed rare amplification limited to <1% of cases. An unexpected observation was that 13 cases (6.3%) showed coamplification of multiple RTKs. The most common was coamplification of *EGFR* and *PDGFRA* (five cases). *EGFR* was simultaneously coamplified with *EPHB3*, *ERBB3*, *INSRR*, *MET*, and *NTRK1*, each in one case. One case showed coamplification of numerous RTKs, including *EPHA8*, *EPHB2*, *FGFR2*, and *PDGFRA*. One case showed coamplification of *MET* and *PDGFRA*. Overall, *EGFR*, *PDGFRA*, and *MET* were the most commonly coamplified RTKs (Figure 1A; Figure S1). To confirm the presence of coamplification, we were able to obtain unstained slides from a single original TCGA case (TCGA-02-0024) with *MET* and *PDGFRA* amplification, and we performed fluorescence in situ hybridization (FISH) for *EGFR*, *MET*, and *PDGFRA*, which showed coamplification of *PDGFRA* and *MET* within the same tumor cells (Figure 1B).

Mosaic Amplification of Multiple RTKs within GBM

Due to possible major clinical implications of the coamplification of multiple RTKs in single tumors, we performed simultaneous FISH for *EGFR*, *MET*, and *PDGFRA* on our cohort of 350 GBMs. In total, we have observed 16 GBMs (4.5%) with more than one amplified RTK. Surprisingly, and unlike TCGA-02-0024, these multiple RTK amplifications were not present in the same tumor cell, but were present in distinct intermingled subpopulations of tumor cells (Figure 2). Twelve tumors contained two distinct subpopulations of tumor cells, each with mutually exclusive amplification events, including seven tumors with *EGFR* and *PDGFRA*-amplified subpopulations (Figure 2A), three tumors with *MET* and *EGFR* populations (Figure 2B), and two tumors with *PDGFRA* and *MET* populations (Table S1). Furthermore, four tumors in our study harbored mutually exclusive amplified subpopulations of all 3 genes *EGFR*, *MET*, and *PDGFRA*. These distinct subpopulations did not cluster in single areas, but were intermingled throughout the tumors.

Given the unusual nature of these mosaic tumors, there was concern that they may in fact represent rare tumors with very high levels of genome-wide chromosomal instability such as the recently described chromothripsis phenomenon (Stephens et al., 2011). In such an instance, multiple amplifications may represent "passenger" events (i.e., reflect genomic instability with little impact on the growth of the tumor). We thus employed a genome-wide copy number assessment (array comparative genomic hybridization [aCGH]) on three of these mosaic tumors for which we had DNA of sufficient quantity and quality. In two cases known to harbor three RTK populations by FISH, we observed coamplification of only two subpopulations each by aCGH—*EGFR* and *MET* in one (Figure 3A) and *PDGFRA* and *MET* in the other (Figure 3B). A third case showed only *EGFR* amplification, failing to detect the expected minor population of *PDGFRA*-amplified cells (Figure 3C). Thus, genome-wide copy number assays are not as sensitive as FISH at detecting the minor subpopulations. In all three cases analyzed by aCGH, the amplicons were focal, encompassing only the immediate genomic regions surrounding the genes of interest, and importantly there was no apparent unusually high level of genomic instability. We did not detect any other focal amplification events involving known cancer genes; however, all three cases had *CDKN2A* deletion.

Functionality of Subpopulations with Amplifications of Different RTK

To further investigate the relevance of these amplification events for tumor growth, we assessed whether each subpopulation was actively proliferating and whether gene amplifications resulted in overexpression of the corresponding protein. We performed combined immunofluorescence (IF)-FISH and observed that

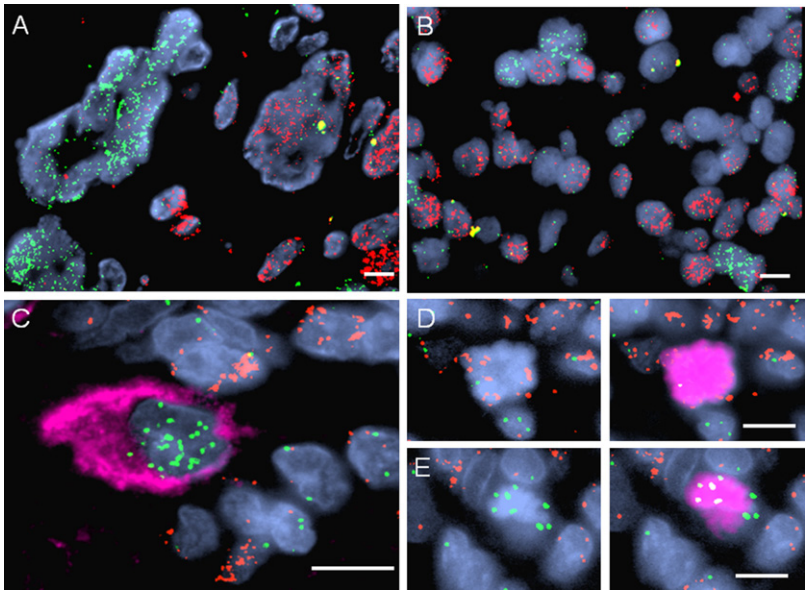

Figure 2. Mosaic Amplification of RTKs

(A) Two distinct populations of tumor cells with mutually exclusive amplification of *EGFR* (red) or *PDGFRA* (green).

(B) Intermingled subpopulations with mutually exclusive *EGFR* (red) or *MET* (green) amplification.

(C) Expression of MET protein (pink) was limited to cells with *MET* amplification (green). *EGFR*-amplified cells (red) are negative.

(D and E) Proliferation marker phospho-histone H3 (pink) highlights proliferating *EGFR*-amplified (red) cells and *MET*-amplified tumor cells (green) in the same tumor (right panels overlap). Scale bars, 20 μm.

each of the cells with amplification of a specific RTK produced overexpression of the respective protein only; for example, tumor cells with *MET* amplification showed MET overexpression compared to *EGFR*-amplified tumor cells, which lacked MET overexpression (Figure 2C). To prove that each amplified subpopulation was actively proliferating, we performed IF-FISH with anti-phospho-histone H3 (M phase marker) antibodies. Within each tumor, all RTK subpopulations were mitotically active, as highlighted by the positivity of cells with each of the possible gene amplifications for phospho-histone H3 expression (Figures 2D and 2E).

Subpopulations with Different RTK Amplifications Are Derived from the Same Precursor

Even though each tumor presented clinically as a single brain mass, we sought to exclude the possibility of a "collision" tumor, where multiple independent primary tumors are present in the same anatomic location. To demonstrate that amplified subpopulations developed from the same precursor, we attempted to show that within single tumors, the RTK-amplified subpopulations shared a common early precursor genetic alteration such as homozygous deletion of *CDKN2A* or *TP53* mutation. In four tumors, we observed homozygous loss of *CDKN2A* by FISH, and importantly, the deletions were in all RTK-amplified subpopulations, including all three subpopulations in one case and both subpopulations in three other cases (Figures 4A–4C). Homozygous *CDKN2A* loss was also observed by our aCGH (Figures 3A–3C) as well as in four out of seven TCGA cases with multiple amplified RTKs (Figure 1B). In seven cases, we did not observe homozygous deletion in any of the subpopulations. Two of the cases were strongly positive for TP53 protein expression consistent with TP53 mutation, which was detectable by IF-FISH in all amplified subpopulations (Figures 4D and 4E). We completely sequenced *TP53* from one of the cases with sufficient material, which showed that only a single mutation 422 G > A (C141Y) was detectable in the tumor (Figure 4F). In all cases the *CDKN2A* and *TP53* genotypes were concordant in each of the subpopulations. Statistical analysis shows that one can reject the null hypothesis that the subpopulations originated independently (i.e., that *CDKN2A* homozygous deletions and *TP53* mutations jointly occurred independently among subpopulations) (p value, 5.52×10^{-7}). This strongly supports our hypothesis that subpopulations with different RTK amplifications are derived from the same precursor, and thus can be considered subclones.

Microscopic Distribution of Mosaic Subclones

To quantitate the degree of mosaicism of these subclones, we scored the number of each of four possible cell populations (*EGFR*, *MET*, *PDGFRA*, or none) (Figure 4G). The ratios of amplified subclones varied broadly among tumors, with some tumors showing dominant *EGFR*, *MET*, or *PDGFRA* populations, and other tumors showing evenly distributed percentages of each. Although most of the cases in this study were small biopsies, we had access to a complete brain autopsy for case 8, a patient with GBM who died untreated 33 days after diagnosis, allowing us to perform a detailed microscopic analysis of mosaicism in a single case. The patient presented with a main left parietal tumor and a second abnormality in the right cingulate gyrus. Gross examination of the brain showed extensive tumor involvement bilaterally, with a large left parietal mass extending into the occipital and frontal lobes and the additional right cingulate mass (Figure 5A). FISH studies of tissue sections showed the presence of *EGFR*- and *PDGFRA*-amplified subclones in an approximately 60:40 ratio within the main tumor mass (Figures 5B and 5C). However, the infiltrating portion contained exclusively *EGFR*-amplified cells, which included cells within the corpus callosum and comprised the entire tumor cell population of the right cingulate mass (Figures 5D–5F, respectively). *EGFR*-amplified cells were again found in the infiltrating edges (Figure 5G), extending into the grossly normal right temporal lobe white matter (Figure 5H). Whereas *PDGFRA* amplified cells were numerous in the large primary left parietal mass, they were not found in the infiltrating tumor in either the left or right hemisphere.

Correlation with Clinical Parameters

For 12 patients, clinical data were available for review. There was no apparent association with clinico-pathologic parameters, including tumor site, sex, age, O6-methylguanine

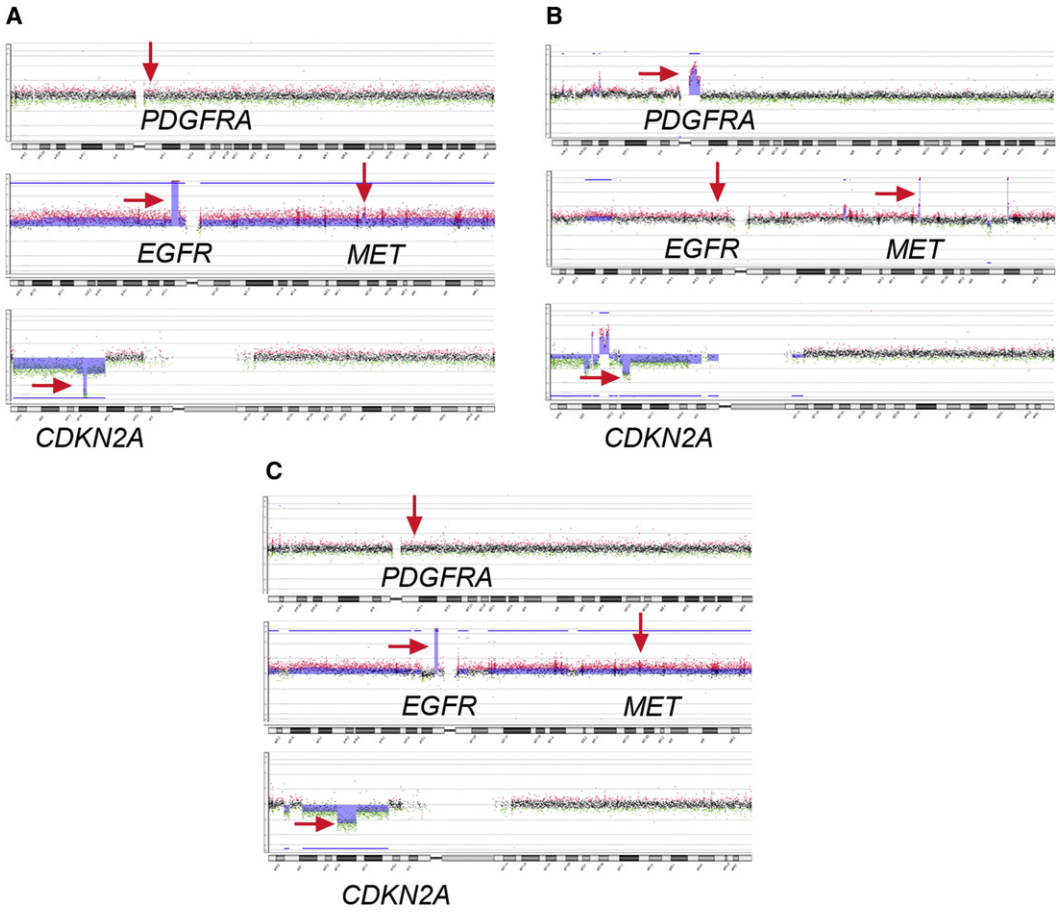

Figure 3. Selected View of aCGH Analyses (Chromosomes 4, 7, and 9) from Three Cases
(A) No copy number change of *PDGFRA*, high-level gain of *EGFR*, and borderline gain of *MET*.
(B) High-level gain of *PDGFRA* and *MET*, but no change for *EGFR*.
(C) High-level amplification of *EGFR*, but no change for *PDGFRA*, which showed amplifcation by FISH. *CDKN2A* shows homozygous loss in all three cases.

methyltransferase (MGMT) status, response to therapy, or survival (Table S1; Figure S2). The median overall survival was 473 days, which is in line with the expected survival for GBM patients, though numbers remain too small for definitive conclusions about clinical significance of this finding.

Our findings are limited to GBM; however, we also identified a case of a salivary duct carcinoma with amplification of *ERBB2* and *PDGFRA* in separate subclones (Figure S2), which suggests that the presence of multiple driver genes might not be unique for GBM but could be a more common and underappreciated phenomenon of tumor heterogeneity.

DISCUSSION

We observed an example of tumor genetic heterogeneity in primary human glioblastomas in which up to three different focal RTK amplifications define independent clonal populations possessing proliferative capacity and functional expression of the corresponding RTK protein. The subclones within each tumor invariably shared common *CDKN2A* deletion status or *TP53* status, suggesting that the different RTK populations arose from a single precursor. These observations have implications for our basic understanding of human tumor biology, especially with regard to clonal evolution, the role of gene amplifications in this evolutionary process, and the refining of definitions of tumor driver genes.

Carcinogenesis is an evolutionary process that gives rise to malignant clones via the process of natural selection and adaptation. The fact that genetic/genomic instability is a hallmark of malignancy (Hanahan and Weinberg, 2011) implies that there is some degree of genetic heterogeneity in all cancers, and this intratumor heterogeneity allows for genetic diversity that plays a crucial role in tumor cell evolution and selection of the clones with highest proliferative advantage. This is especially important in the adaptive responses to certain selection pressures such as hypoxia, metabolic stress, chemotherapy, or radiotherapy (Gerlinger and Swanton, 2010). Since nearly all of the mosaic tumors analyzed here were initial biopsies/resections without prior chemo-radiation, and importantly without exposure to prior RTK inhibitors, we are probably observing genetic adaptions that are purely proproliferation or perhaps protective against metabolic stress. We have previously described tumor heterogeneity with respect to *EGFR* amplification in glioblastoma, where *EGFR*-amplified cells are often enriched at the invading edge of

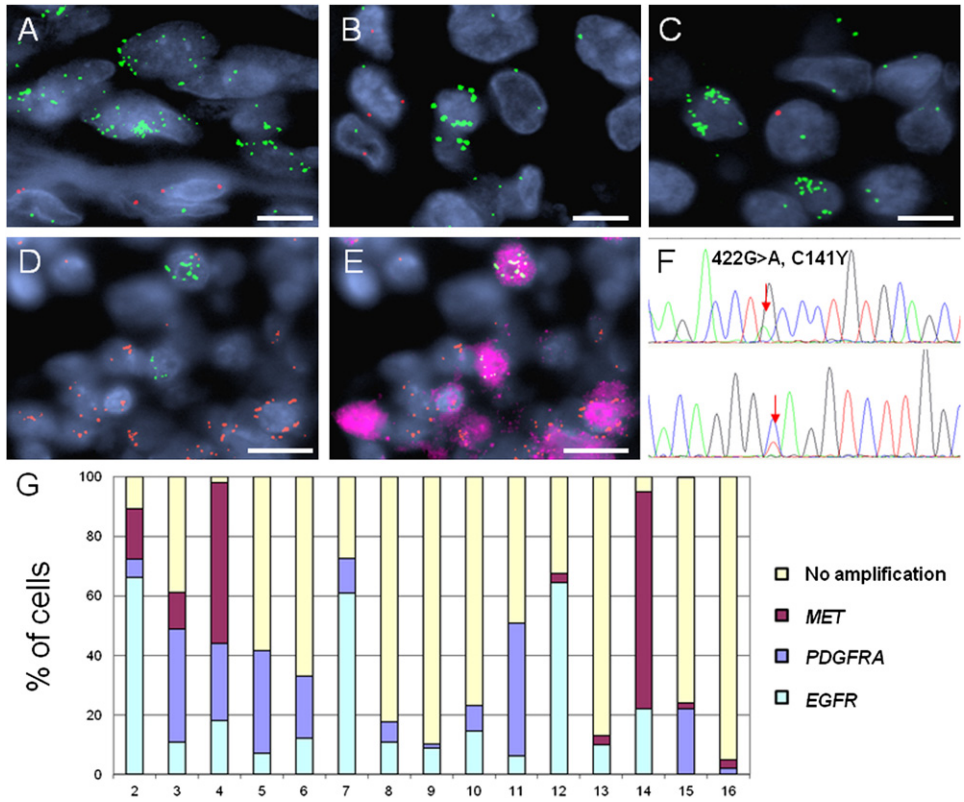

Figure 4. Subpopulations with RTK Amplifications

(A–C) All subpopulations with RTK amplifications share the same mutation and are likely derived from the same precursor. Homozygous loss of *CDKN2A* (red) was seen in tumor cells with RTK amplification (green) in *EGFR*-amplified (A), *MET*-amplified (B), and *PDGFRA*-amplified (C) subpopulations within the same tumor shown.

(D and E) Both *EGFR*-amplified (red) and *MET*-amplified (green) subpopulations (D) show accumulation of TP53 protein (pink), suggesting TP53 mutation (E, overlap).

(F) Sanger sequencing of the *TP53* gene reveals only one mutation (422G>A, C141Y). Forward and reverse tracings are shown.

(G) Ratios of amplified subpopulations in 15 of 16 GBMs with sufficient tissue for quantification. Case numbers 2-4 show three populations of amplified cells, one *EGFR* dominant, one *PDGFRA* dominant, and one *MET* dominant. Cases 5-11 show variable populations of *EGFR*- and *PDGFRA*-amplified cells interspersed within tumor population with no amplification. Cases 12-14 show tumors with a mixture of *EGFR*- and *MET*-amplified subpopulations. Cases 15 and 16 show a mixture of *PDGFRA* and *MET*. Scale bars, 20 μm.

tumors (Okada et al., 2003). This likely reflects cellular adaptation within a specific niche and suggests that within RTK mosaic tumors that each of the three populations may be filling distinct niches within the tumor microenvironment. Thus, whereas the three subclones are defined by amplification and expression of the related RTKs *EGFR*, *PDGFRA*, and *MET*, the proteins might have distinct effects on downstream signaling pathways in each cell population. The fact that there are no fibroblasts in GBMs might suggest that the growth and support signals known to be provided by the tumor stoma in epithelial tumors may themselves be provided in GBMs in part by different populations of tumor cells via paracrine and autocrine signaling.

The coexistence of intermingled functional and actively dividing *EGFR*, *MET*, and *PDGFRA*-amplified subclones strongly supports that there is ongoing selection pressure for the growth of each subclone. The aCGH data indicate that these mosaic tumors are not characterized by unusually high levels of genomic instability; nonetheless, we cannot entirely exclude that there is some stochastic instability at the *EGFR*, *MET*, and *PDGFRA* loci. The stable coexistence of multiple clones in these tumors could be explained by near-identical fitness of each of the subclones, which are outgrowing the precursor population but not outgrowing each other. A more intriguing possibility, however, is that the selection may be strongest for the population of subclones together as a cooperative group of genetically diverse clones. This tumor cell-tumor cell interaction can be modeled as the cooperation of different tumor cells rather than a competition for the most viable clone (Bach et al., 2001).

The mosaic amplification of RTKs is present in approximately 5% of GBMs, and it is possible that this observation is the tip of the iceberg in terms of driver gene heterogeneity in cancer. We suspect that this observation has not been made previously because of the technical limitations of whole genome copy number analysis. Although DNA microarrays are effective at detecting high-level amplification events in pure tumor populations, as we observed here they will likely have difficulty detecting mosaic populations whose copy number elevations are diluted out both by mosaic nonamplified cells and contaminating

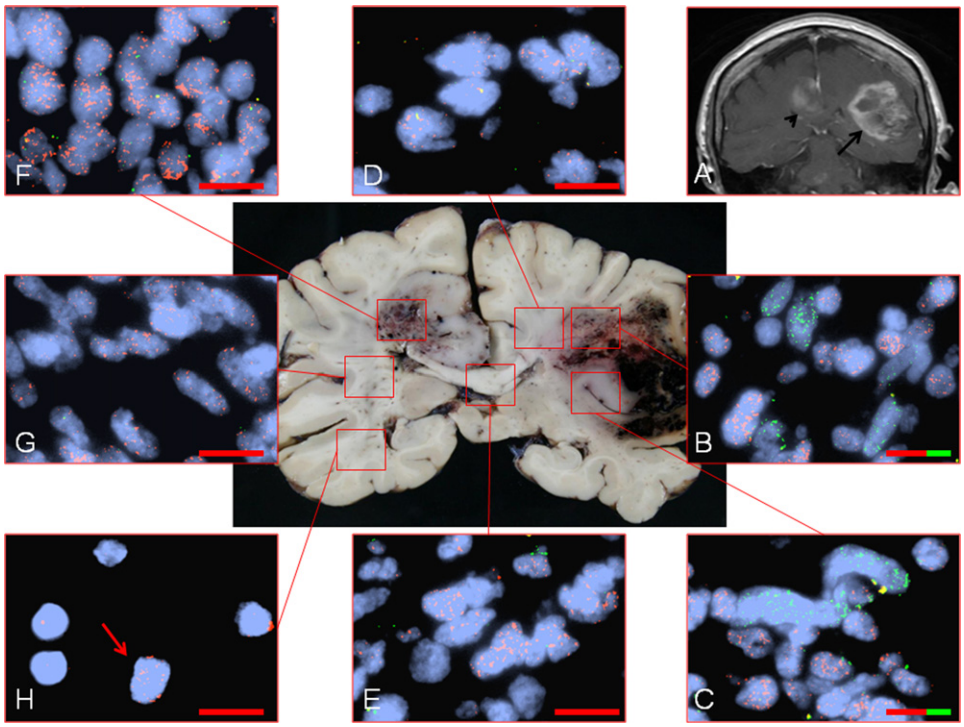

Figure 5. Autopsy Study of a Mosaic GBM Case

(A) Magnetic resonance imaging with contrast shows a large primary tumor with ring enhancement in the left parietal lobe (arrow) and a smaller secondary lesion in the right cingulate gyrus (arrowhead).

(B and C) The main parietal tumor mass shows a mixture of cells with either *EGFR* (red) or *PDGFRA* (green) amplification.

(D and E) The invasive edge of the main tumor (D) and corpus callosum (E) are infiltrated by GBM cells composed exclusively of cells with *EGFR* amplification.

(F–H) The second mass in the right cingulate gyrus is also composed of *EGFR*-amplified cells (F), which infiltrate (G) into the white matter of the right temporal lobe (H, arrow). *EGFR:PDGFRA* subclones in the main tumor mass are in an approximately 60:40 ratio. Colors represent the percentage of *EGFR*-amplified (red) or *PDGFRA*-amplified (green) subclones in each section. Scale bars, 40 μm. See also Figure S2 and Table S1.

normal nonneoplastic cells. Thus, FISH or other in situ techniques are currently the only method to detect such mosaicism (Navin et al., 2010). However, as techniques for the assessment of genetic alterations in single cells develop, we will observe many more examples of this class of tumor (Navin et al., 2011).

Our study raises important issues regarding targeted therapies, including that multiple RTK-targeted therapies may be required in tumors with mosaic driver gene amplification. However, if the coexistence of different populations provides a survival benefit, disrupting any one interaction might collapse the mutual relationship and thus inhibit the growth of the tumor overall. EGFR inhibitors have had at best modest efficacy in GBM patients, and any responses have been unrelated to *EGFR* amplification (Nicholas et al., 2011; Yung et al., 2010). The lack of response is surprising given the very high level of *EGFR* amplification in many tumors, and it is possible that genetic heterogeneity could contribute to this refractoriness.

Our observations underscore the need to clearly define the use of the term ''driver'' mutation. Driver mutations in general can be defined as those that provide a selective growth advantage for tumor cells and are likely good targets for drug development (Haber and Settleman, 2007). Drivers can be divided into early (or tumor initiating) and late (or progression) drivers. Our observations confirm that loss of *CDKN2A* (Tunici et al., 2004) precedes high-level amplification of RTKs such as *EGFR* (Attolini et al., 2010) and therefore acts as an early driver in primary/de novo GBM, and would be expected to be present in all tumor cells. Amplifications of *EGFR*, *PDGFRA*, and *MET*, as progression drivers, are often heterogeneous within single tumors.

In summary, we describe a unique subtype of human brain tumor driven by multiple intermixed populations of cells each with amplification of a different receptor tyrosine kinase. This observation suggests that RTK amplifications are late events which are heterogeneously distributed. There are potentially major implications of mosaic RTK amplification for the development of targeted therapies for malignant brain tumors.

EXPERIMENTAL PROCEDURES

Patients and Tumor Specimens

Analyses were performed on 350 archival specimens of glioblastoma, World Health Organization rade IV, seen at the Department of Pathology, Massachusetts General Hospital, from 2009 to 2011. Approval from the Dana-Farber/Harvard Cancer Center Institutional Review Board was obtained prior to the initiation of the study (protocol #2010P002871), and because we used discarded tissue only, a waiver of informed consent was received. Formalin-fixed, paraffin-embedded brain biopsy tissues were stained with routine hematoxylin and eosin stain, and cases were reviewed by two neuropathologists (M.S., D.N.L.). The Cancer Genome Atlas project data were

analyzed via cBio Cancer Genomics Portal (http://www.cbioportal.org) provided by Memorial Sloan-Kettering Cancer Center.

Molecular Analysis

FISH was performed with *EGFR* (CTD-2113A13 Spectrum Red or Green, Invitrogen Nick translation Kit), *MET* (CTB-1013N12 Spectrum Green, Invitrogen Nick translation Kit), *PDGFRA* (RP11-58C6 Spectrum Red or Green, Invitrogen Nick Translation Kit), *CDKN2A* (RP11-149I2 Spectrum Red, Invitrogen Nick translation Kit) probes. In cases where minimum of 1000 tumor cells were present (cases 2-16), populations with and without amplification were quantified independently by three observers (L.F., M.S., and B.H.Z.). For indirect IF staining, we used the following antibodies: mouse anti-EGFR (1:50, Santa Cruz Biotechnology), rabbit anti-MET (1:100, Abcam), rabbit anti-PDGFR-alpha (1:100, Abcam), rabbit anti phospho-histone H3 (1:100, Abcam), and mouse anti-TP53 (1:15, Santa Cruz Biotechnology). Pressure-cooker antigen retrieval was performed by heating tissue sections in Borg Decloaker solution (Biocare Medical, Concord, CA) for 3 min followed by cooling sections to room temperature. Slides were washed and incubated in PBS buffer for 5 min. Slides were then incubated in Avidin D for 20 min, Biotin for 20 min, primary antibody for 60 min, biotinylated secondary antibody for 30 min, and streptavidin-conjugated fluorophore for 30 min between washes in PBS. Slides were dehydrated in ethanol and dried in a 65°C oven for 5 min. FISH was performed with a mix of 2-3 probes (3 μL/slide) applied to the slides, followed by denaturation of the probe and target at 80°C for 5 min and overnight hybridization at 37°C. Two 2 min posthybridization washes in 2× SSC were performed with a 72°C water bath and one 1 min wash in 2× SSC was performed at room temperature. Nuclei were counterstained with 4',6-diamidino-2-phenylindole. Images were acquired with an Olympus BX61 fluorescent microscope equipped with a charge-coupled device camera and analyzed with Cytovision software (Applied Imaging, Santa Clara, CA).

For aCGH studies, genomic DNA was extracted from formalin-fixed, paraffin-embedded tissue using the QIAamp Blood Mini Kit using a modified protocol incorporating deparaffinization and protease digestion (QIAGEN, Valencia, CA). Genome-wide copy number alterations were analyzed by array comparative genomic hybridization using the Agilent 4x180k CGH + SNP microarray (Santa Clara, CA) containing 110,712 copy number probes covering both coding and noncoding human sequences with an overall median probe spacing of 25.3 kb (5 kb in regions defined by the International Standards of Cytogenomic Arrays). Briefly, 1.5 μg of NA12891 European male genomic control DNA (Corriell Institute, Camden, NJ) and 1.5 μg of tumor DNA were heat-treated at 95°C for 5 min. Control and tumor DNA were labeled by random priming with CY3 and CY5 deoxyuridine triphosphate dyes, respectively, using the Agilent Genomic DNA Enzymatic Labeling Kit. The labeled DNA were purified with the Millipore Amicon 30 kDa centrifugal filter device (Billerica, MA) and mixed in equal proportion for hybridization to the array in the presence of Cot-1 DNA (Invitrogen, Carlsbad, CA) using the Agilent Oligo aCGH Hybridization Kit. Hybridization steps included 3 min denaturation at 95°C, prehybridization for 30 min at 37°C, and hybridization for 35-40 hr at 65°C. Following hybridization, the slides were washed with Agilent Oligo Array CGH Wash Buffer 1 and Buffer 2, at room temperature for 5 min and at 37°C for 1 min, respectively. The slides were washed in acetonitrile (Sigma, St. Louis, MO) for 10 s. The final wash was performed in Agilent stabilization and drying solution for 30 s. Washed slides were scanned using the Agilent G2565CA Microarray Scanner. Microarray TIFF (.tif) images were processed and analyzed with Agilent CytoGenomics v1.5 software. Copy number aberration calls were made with a minimum regional absolute average log base 2 ratio of 0.25 and minimum contiguous probe count of 5. All array data were also manually reviewed for subtle copy number changes not detected by the software.

Statistical Analysis

We tested our hypothesis that subclones within each mosaic tumor are derived from the same precursor versus arising as independent tumors using *CDKN2A* (*p16*) homozygous deletion and *TP53* mutation data. The p value is defined to be the probability of the observed genotype changes, or changes that are equally as "extreme," under the assumption of their independence across subclones and relative to the alternative hypothesis that there is a single event for each tumor. The observed data that we treated as fixed in the analysis were: 13 subjects, 1 with three subclones, 12 with two subclones, and thus 27 subclones, 9 with homozygous p16 deletion only (p16+/*TP53*−), 14 with no homozygous p16 deletion and no *TP53* mutation (p16−/*TP53*−), and 4 with *TP53* mutation only (p16−/*TP53*+). Conditional on these data, the p value is the probability of observing any assortment of these results such that the subclones in each subject have the same results, and assuming independence across all subclones. This simplifies to a hypergeometric probability:

$$\frac{\binom{12}{3}\binom{9}{7}}{\binom{27}{9}\binom{18}{14}} = 5.52 \times 10^{-7}$$

The denominator counts the number of ways that the 9 p16+/*TP53*− subclones can be distributed among the 27 subclones, and the 14 p16−/*TP53*− subclones can be distributed among the 18 remaining subclones (there is then no choice for placement of the remaining 4 p16−/*TP53*+ clones). The numerator counts the number of ways the 12 subjects with two clones can be assigned to the three remaining p16+/*TP53*− pairs of subclones (note that the subject with three subclones must be assigned to have all p16+/*TP53*− subclones given the observed data) and the remaining 9 subjects can be assigned to the 7 p16−/*TP53*− pairs of subclones (there is then no choice for placement of the remaining 2 p16−/*TP53*+ pairs of subclones). This is equivalent to a 13 × 3 Fisher's exact test for independence between subjects and subclones with regard to p16/*TP53* status. Survival was estimated using the Kaplan-Meier method.

ACCESSION NUMBERS

Array CGH data have been deposited in Gene Expression Omnibus (GEO, http://www.ncbi.nlm.nih.gov/geo/) and are accessible under accession number GSE33483.

SUPPLEMENTAL INFORMATION

Supplemental information includes two figures and one table and can be found with this article online at doi:10.1016/j.ccr.2011.11.005.

Received: June 14, 2011
Revised: October 11, 2011
Accepted: November 7, 2011
Published online: December 1, 2011

REFERENCES

Attolini, C.S., Cheng, Y.K., Beroukhim, R., Getz, G., Abdel-Wahab, O., Levine, R.L., Mellinghoff, I.K., and Michor, F. (2010). A mathematical framework to determine the temporal sequence of somatic genetic events in cancer. Proc. Natl. Acad. Sci. USA *107*, 17604–17609.

Bach, L.A., Bentzen, S.M., Alsner, J., and Christiansen, F.B. (2001). An evolutionary-game model of tumour-cell interactions: possible relevance to gene therapy. Eur. J. Cancer *37*, 2116–2120.

Cancer Genome Atlas Research Network. (2008). Comprehensive genomic characterization defines human glioblastoma genes and core pathways. Nature *455*, 1061–1068.

Gerlinger, M., and Swanton, C. (2010). How Darwinian models inform therapeutic failure initiated by clonal heterogeneity in cancer medicine. Br. J. Cancer *103*, 1139–1143.

Haber, D.A., and Settleman, J. (2007). Cancer: drivers and passengers. Nature *446*, 145–146.

Hanahan, D., and Weinberg, R.A. (2011). Hallmarks of cancer: the next generation. Cell *144*, 646–674.

Jain, R.K., di Tomaso, E., Duda, D.G., Loeffler, J.S., Sorensen, A.G., and Batchelor, T.T. (2007). Angiogenesis in brain tumours. Nat. Rev. Neurosci. *8*, 610–622.

Joensuu, H., Puputti, M., Sihto, H., Tynninen, O., and Nupponen, N.N. (2005). Amplification of genes encoding KIT, PDGFRalpha and VEGFR2 receptor

tyrosine kinases is frequent in glioblastoma multiforme. J. Pathol. *207*, 224–231.

Louis, D.N., Ohgaki, H., Wiestler, O.D., and Cavenee, W.K. (2007). World Health Organization classification of tumors of the Central Nervous System (Lyon: IARC Press).

Marusyk, A., and Polyak, K. (2010). Tumor heterogeneity: causes and consequences. Biochim. Biophys. Acta *1805*, 105–117.

Navin, N., Krasnitz, A., Rodgers, L., Cook, K., Meth, J., Kendall, J., Riggs, M., Eberling, Y., Troge, J., Grubor, V., et al. (2010). Inferring tumor progression from genomic heterogeneity. Genome Res. *20*, 68–80.

Navin, N., Kendall, J., Troge, J., Andrews, P., Rodgers, L., McIndoo, J., Cook, K., Stepansky, A., Levy, D., Esposito, D., et al. (2011). Tumour evolution inferred by single-cell sequencing. Nature *472*, 90–94.

Nicholas, M.K. (2007). Glioblastoma multiforme: evidence-based approach to therapy. Expert Rev. Anticancer Ther. *7* (12, Suppl), S23–S27.

Nicholas, M.K., Lukas, R.V., Chmura, S., Yamini, B., Lesniak, M., and Pytel, P. (2011). Molecular heterogeneity in glioblastoma: therapeutic opportunities and challenges. Semin. Oncol. *38*, 243–253.

Okada, Y., Hurwitz, E.E., Esposito, J.M., Brower, M.A., Nutt, C.L., and Louis, D.N. (2003). Selection pressures of TP53 mutation and microenvironmental location influence epidermal growth factor receptor gene amplification in human glioblastomas. Cancer Res. *63*, 413–416.

Puputti, M., Tynninen, O., Sihto, H., Blom, T., Mäenpää, H., Isola, J., Paetau, A., Joensuu, H., and Nupponen, N.N. (2006). Amplification of KIT, PDGFRA, VEGFR2, and EGFR in gliomas. Mol. Cancer Res. *4*, 927–934.

Stephens, P.J., Greenman, C.D., Fu, B., Yang, F., Bignell, G.R., Mudie, L.J., Pleasance, E.D., Lau, K.W., Beare, D., Stebbings, L.A., et al. (2011). Massive genomic rearrangement acquired in a single catastrophic event during cancer development. Cell *144*, 27–40.

Tunici, P., Bissola, L., Lualdi, E., Pollo, B., Cajola, L., Broggi, G., Sozzi, G., and Finocchiaro, G. (2004). Genetic alterations and in vivo tumorigenicity of neurospheres derived from an adult glioblastoma. Mol. Cancer *3*, 25.

Wullich, B., Müller, H.W., Fischer, U., Zang, K.D., and Meese, E. (1993). Amplified met gene linked to double minutes in human glioblastoma. Eur. J. Cancer *29A*, 1991–1995.

Yachida, S., Jones, S., Bozic, I., Antal, T., Leary, R., Fu, B., Kamiyama, M., Hruban, R.H., Eshleman, J.R., Nowak, M.A., et al. (2010). Distant metastasis occurs late during the genetic evolution of pancreatic cancer. Nature *467*, 1114–1117.

Yip, S., Miao, J., Cahill, D.P., Iafrate, A.J., Aldape, K., Nutt, C.L., and Louis, D.N. (2009). MSH6 mutations arise in glioblastomas during temozolomide therapy and mediate temozolomide resistance. Clin. Cancer Res. *15*, 4622–4629.

Yung, W.K., Vredenburgh, J.J., Cloughesy, T.F., Nghiemphu, P., Klencke, B., Gilbert, M.R., Reardon, D.A., and Prados, M.D. (2010). Safety and efficacy of erlotinib in first-relapse glioblastoma: a phase II open-label study. Neuro-oncol. *12*, 1061–1070.